An Innovative Pick and Place Robotic Arm System Using an Atmega328 Microcontroller with Escalating Stabiity

[1]Olaoluwa D. Aladetola, [2*]Najeem O. Adelakun,

[3]Ayodeji O. Ajayi

[1]Department of Electrical Electronics Engineering, Federal Polytechnic, Ilaro, Ogun State, Nigeria
[2]Engineer/Researcher, Federal College of Education Iwo, Osun State, Nigeria*
[3]Technical Support Engineer, Powerex Limited, Omole Phase II, Lagos State, Nigeria
*ollyboi999@yahoo.com[1], *adelakunnajeem@gmail.com[2], silverdammy@gmail.com[3]*

Indian Journal of Advances in

Science Engineering and Technology

Vol 1 No 2 2022: 39-52

IJASET

Original Article

An Innovative Pick and Place Robotic Arm System Using an Atmega328 Microcontroller with Escalating Stabiity

[1]Olaoluwa D. Aladetola, [2*]Najeem O. Adelakun, [3]Ayodeji O. Ajayii

[1]Department of Electrical Electronics Engineering, Federal Polytechnic, Ilaro, Ogun State, Nigeria

[2]Federal College of Education Iwo, Osun State, Nigeria*

[3]Powerex Limited, Omole Phase II, Lagos State, Nigeria

*ollyboi999@yahoo.com[1], *adelakunnajeem@gmail.com[2], silverdammy@gmail.com[3]*

Abstract

It is well known that the pick and place mechanism can take the role of human arms, particularly in industrial settings, and that it is more accurate and faster at performing jobs. The mechanism created in this study is an inexpensive device controlled by sensors that can propel items swiftly. The proposed system simulates the behavior of a human in accomplishing a specific industrial job with increased stability than the existing designs. Ultrasonic sensors were used to sense anything for picking and positioning in industries, together with servo motors, an Atmega328 Arduino microprocessor, and light steel iron for the frames. The system's stability as derived from the theoretical equations is verified using Matlab software. The elevated stability was achieved utilizing a step input signal that is a type zero system. The observability, controllability, polar plot, and bode were also established. The phase difference for the bode plot is 173 degrees, and the system rise time is 1.01 seconds. The findings demonstrate the device's escalated stability and dependability, which will increase productivity and lower production costs when used by the industry. The device can be usefully utilized in an environment that is life-threatening to human beings. The limitation of the proposed system is that it is stationary and can be used only to move an object along a conveyor belt; it is not mobile. Nevertheless, it outperforms current ones economically. It is more affordable, exceedingly dependable, repeatable, and steady.

Keywords: **Arduino, Armature Dc Servo Motors, Robotic Arm, Atmega328 Microcontroller, Pick and Place Robots**

1. Introduction

Technological growth and the need for easy matching devices gives rise to persistent development, Scientist and engineers are mostly premiers in raising new technologies [1]. A robot can be defined as an electromechanical device that moves and performs automated tasks according to a pre-defined program by direct human supervision [2 – 4]. It should be highlighted that robots can complete activities that, in terms of difficulty, precision and speed, cannot be completed by humans [5, 6]. The Czech word "robota," which signifies *forces* or *labor*, is where the term "robot" originated and it was first used in 1921 by Karel Capek [7, 8]. Robots are used in nearly all human labour, mostly in jobs that are dangerous or hazardous for labourers [9, 10].

A robotic arm, as shown in Figure – 1, is a programmable mechanical device that can replace the functions of a human arm; it performs simple translational and rotational motion, which has an end effector that performs a specific function [11, 12]. Similarly, the device is a mechanized pick-and-place robot arm that grasps objects exactly, put it at the appropriate location, and reach it within a specific domain or span of space [13]. This method is employed to lift objects and perform activities that demand for utmost focus, exactitude, and maybe recursion [14, 15]. Industrial arms performance has increased over the years with the advent of microcontrollers and programming developments [16, 17], which has given rise to massive transformation in the robotic industry [12, 18, 19]. As a result, in order to create an effective design for a robot, concepts, methodologies, congitive science and artificial intelligence are crucial.

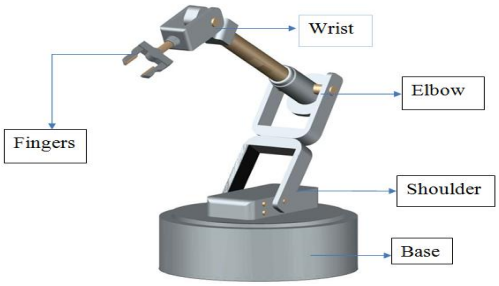

Figure – 1: Two-link Robotic Manipulator System

2. Mathematical Modelling of the System

The Rotational Double Inverted Pendulum (RDIP) used consists of two vertical pendulums and a servo-driven horizontal base arm designated as Link – 1 in Figure – 2 and the RDIP uses the Euler-Lagrange (E-L) function model [20, 21].

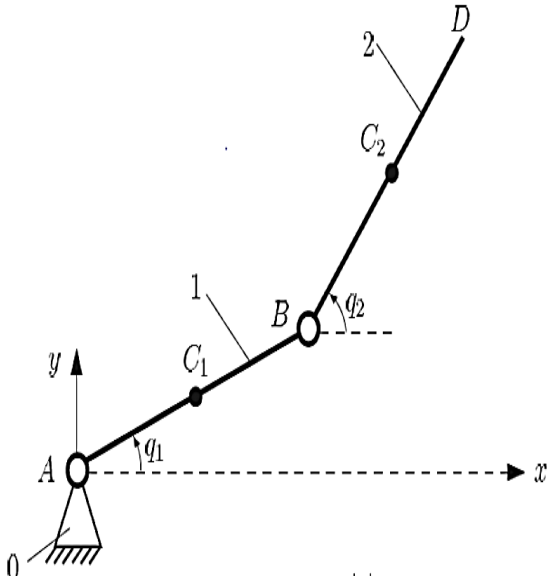

Figure – 2: Structure -link robotic manipulator system

The linkages' mass centres are identified by

^{c_1} $(x^{c_1}; y^{c_1}; 0)$ *and* ^{c_2} $(x^{c_2}; y^{c_2}; 0)$ (1)

Where "n" denotes the number of joints with freedom of single degree and moving connections, respectively, and ^{c_A} is the quantity of joints with freedom of two degrees. The properties of dual pendulum

are as n = 2; c_1 = 2; c_A= 0. Additionally, the system has two generalised coordinates, M = 2, and of freedom with two degrees.

The coordinates are chosen as the angles q1 and q2, as illustrated in Figure – 2. Resolving Figure – 2 into vector quantities taking into consideration of i and j components and the center's direction vector of the mass c_1 of the link - 1 gives equations (2) and (3).

$$rc_1 = xc_1 i + yc_1 j \tag{2}$$

Where, the coordinates of c_1 are xc_1 and yc_1,

$$xc_1 = \frac{L_1}{2} cosq_1 \tag{3}$$

$$yc_1 = \frac{L_1}{2} sinq_1 \tag{4}$$

The center's position vector of the mass c_2 of the link - 2

$$rc_2 = xc_2 i + yc_2 j \tag{5}$$

Where, the coordinates of c_2 are xc_2 and yc_2.

$$xc_2 = -L_1 cosq_1 + \frac{L_2}{2} cosq_2 \tag{6}$$

$$yc_2 = L_1 sinq_1 + \frac{L_2}{2} sin\, q_2 \tag{7}$$

The vector of speed of c_2, with respect to time, which is the derivation of the direction vector of c_1 , is given by,

$$V_c = \dot{r}c_1 = \dot{x}c_1 i + \dot{y}c_1 j \tag{8}$$

Where $x_{c_2} = -L_1 sinq_1 \frac{dq_1}{dt} - \frac{L_2}{2} \sin q_2 \frac{dq_2}{dt}$ (9)

$$y_{c_2} = -L_1 cosq_1 \frac{dq_1}{dt} - \frac{L_2}{2} \cos q_2 \frac{dq_2}{dt} \tag{10}$$

The vector of acceleration of C_1 is the location vector's double time-dependent derivative of C_1 is:

$$ac_1 = \ddot{r}c_1 = \ddot{x}c_1 i + \ddot{y}c_1 j \tag{11}$$

$$\ddot{x}_{c_2} = \ddot{r}_{c_2} = -L_1 (sin\, q_1 \ddot{q}_1 + \ddot{q}_1 cosq_1 q_1) - \frac{L_2}{2} (sin\, q_2 \ddot{q}_2 + \ddot{q}_2 cosq_2 q_2) \tag{12}$$

$$\ddot{x}c_2 = -L_1 \ddot{q}_1 sinq_1 - L_1 \dot{q_1}^2 cosq_1 - \frac{L_2}{2} \ddot{q}_2 sinq_2 - \frac{L_2}{2} \ddot{q}_2 cosq_2 \tag{13}$$

$$\ddot{y}c_2 = L_1 \ddot{q}_1 cosq_1 - L_1 \dot{q_1}^2 sinq_1 + \frac{L_2}{2} \ddot{q}_2 sinq_2 - \frac{L_2}{2} {q_2}^2 cosq_2 \tag{14}$$

The links – 1 and 2's angular speed vectors are as follows:

$$w_1 = \dot{q_1} k \; ; \quad w_2 = \dot{q_2} k$$

The links – 1 and 2's angular acceleration vectors are as follows:

$\alpha_1 = \ddot{q_1}k\, \alpha_2 = \ddot{q_2}k$

The forces of weights on link - 1 and link - 2 are determined by the double pendulum's motion governed by Newton-Euler equations as follows:

$G_1 = -M_1 g j\, G_2 = -M_2 g j$

Link – 1's gravitational acceleration with regard to the centre of mass

$c_1\ is\ Ic_1 = \frac{M_1 {L_1}^2}{12}$ (15)

The link – 1's gravitational moment of inertia in relation to the fixed point of revolution A*:*

$I_A = I_C + \frac{M_1}{12} {L_1}^2 = \frac{M_1 {L_1}^2}{3}$ (16)

The link – 2's mass point of inertia in relation to the mass centre C_2:

$Ic_2 = \frac{M_1 {L_1}^2}{12}$ (17)

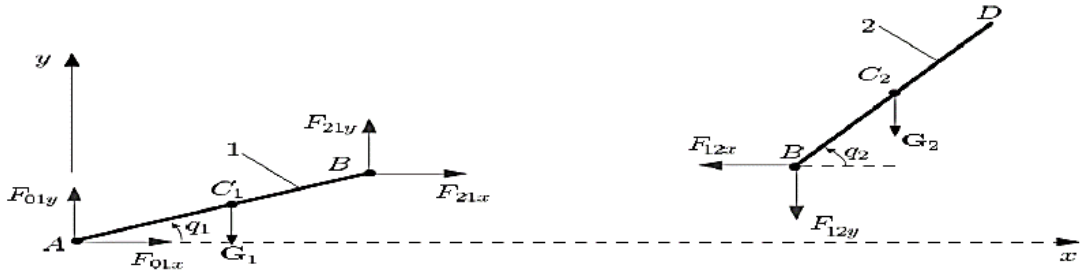

Figure - 3: The Structure of Dynamic 2D Link

2.1. Mathematical Modelling of Link – 1

As taken from Figure - 3, the link – 1 observes the Newton-Euler equations as follows.

$m_1 ac_1 = F_{01} + F_{21}$ (18)

$Ic_1 \alpha_1 = \mathrm{r}C_1 A \times F_{01} + rc_1 B \times F_{21}$ (19)

Where:

The link – 1 and ground 0 at point A have a combined reaction known as F_{01}.

The combined response of link – 1 and link – 2 at location B is F_{21}.

A is the equation of motion

$F_{01} = F_{01}xi + F_{01}yj$ (20)

$F_{21} = F_{21}xi + F_{21}yj$ (21)

The instant of point for link – 1 must be equal the product of the link's gravitational acceleration about the point and its angular acceleration because link – 1 does have a fixed position of rotation at point A. Thus,

$IA\alpha_1 = rAc_1\times + rAB \times F_{21}$ (22)

Resolving Figure – 3 into matrix form Eqn. 23 is given as:

$$A = \begin{bmatrix} i & j & k \\ xc_1 & yc_1 & 0 \\ 0 & -m_1 g & 0 \end{bmatrix} + \begin{bmatrix} i & j & k \\ 0 + xB & yB & 0 \\ F_{21^x} & F_{21^y} & 0 \end{bmatrix} \quad (23)$$

Resolving the matrix from Eqn. 23 and gives Eqn. 24, we get,

$$A = (-m_1 g x c_1 + F_{21} y x B - F_{21} x y B) \quad (24)$$

The link 1 equation of motionis given by:

$$A = (-m_1 g l_{12} + F_{21} y L_1 cosq_1 - F_{21} x L_1 sinq_1) \quad (25)$$

2.2. Mathematical Modelling of Link – 2

The Newton-Euler equations of link – 2 are:

$$m_2 a c_1 = F_{12} + G_2 \quad (26)$$

$$I c_2 \alpha_2 = r c_2 B \times F_{12} \quad (27)$$

Where $F_{12} = -F_{21}$ is the combined reaction Link – 1 and Link – 2 at B. Then we have,

$$m_2 \ddot{x} c_2 = -F_{21^x} \quad (28)$$

$$m_2 \ddot{y} c_2 = -F_{21^x} - m_2 g \quad (29)$$

The reaction component F_{21^x} and F_{21^y} taking into consideration the force acting on each axis from Eqn. 13 and 14 gives 30 and 31.

$$m_2 \left(-L_1 \ddot{q_1} sinq_1 - L_1 \dot{q_1}^2 cosq_1 - \frac{L_2}{2} \ddot{q}_2 sinq_2 - \frac{L_2}{2} cosq_2\right) = -F_{21^x} \quad (30)$$

$$m_2 (-L_1 \ddot{q_1} cosq_1 - L_1 \dot{q_1}^2 sinq_1 + \frac{L_2}{2} \ddot{q}_2 sinq_2 - \frac{L_2}{2} cosq_2) = -F_{21^y} - m_2 g \quad (31)$$

Resolving the sources of the reaction's F_{21x} and F_{21y} components are Eqns. 32 and 33.

$$F_{21}x = m_2 (L_1 \ddot{q_1} sinq_1 + L_1 \dot{q_1}^2 cosq_1 + \frac{L_2}{2} \ddot{q}_2 sinq_2 + \frac{L_2}{2} cosq_2) \quad (32)$$

$$F_{21}y = -m_2 (L_1 \ddot{q_1} cosq_1 + L_1 \dot{q_1}^2 sinq_1 + \frac{L_2}{2} \ddot{q}_2 sinq_2 + \frac{L_2}{2} cosq_2) + m_2 g \quad (33)$$

The F21x and F21y are substituted in Eqns. 32 and 33 to create the following motion equations:

$$\frac{m_2 l_1^2}{3\ddot{q}_1} = \frac{m_1 g l_1}{2cosq} - m_2 (L_1 \ddot{q_1} cosq_1 - L_1 \dot{q_1}^2 \sin q_1 - \frac{L_2}{2} \ddot{q}_2 sinq_2 - \frac{L_2}{2} cosq_2 - g) L_1 cosq_1 -$$

$$m_2 (L_1 \ddot{q_1} sinq_1 + L_1 \dot{q_1}^2 cosq_1 + \frac{L_2}{2} \ddot{q}_2 sinq_2 + \frac{L_2}{2} cosq_2) L_1 sinq_1 \quad (34)$$

$$\frac{m_2 l_1^2}{12 q_2} = \frac{(m_1 l_1)}{2}(L_1\ddot{q}_1 \cos q_1 - L_1\dot{q}_1^2 \sin q_1 - \frac{L_2}{2}\ddot{q}_2 sinq_2 - \frac{L_2}{2} cosq_2 - g)\ cosq_2 +$$

$$\frac{(m_2 l_2)}{2}(L_1\ddot{q}_1 sinq_1 + L_1\dot{q}_1^2 cosq_1 + \frac{L_2}{2}\ddot{q}_2 sinq_2 + \frac{L_2}{2} cosq_2) sinq_1 \quad (35)$$

3. Pick and Place System Modelling

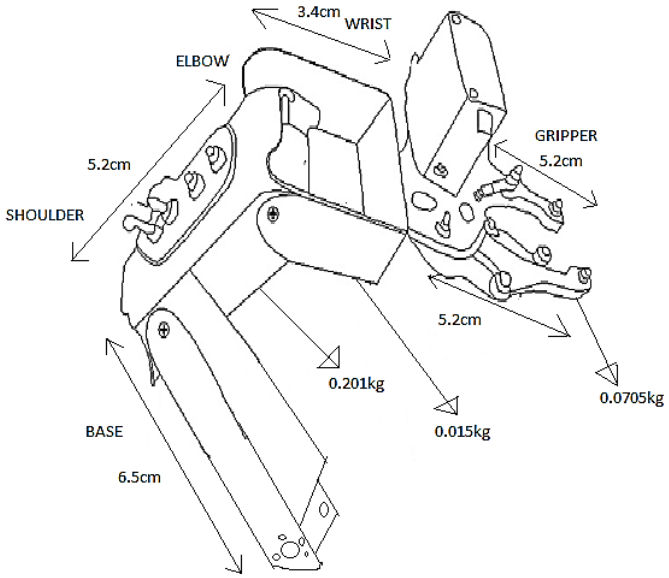

Figure – 4: Mass and Length of the Robotic Arm Links

Figure – 4 shows that:

Mass of servo meter used = 52g = 0.052kg

The length of the shoulder = 7.2cm; with mass of the shoulder link = 0.0201kg

The length of the elbow = 10.4cm; with mass of the elbow link = 0.402kg

The length of the wrist = 3.2cm; with mass of the wrist link = 0.015kg

The length of the gripper = 10.5cm; mass of the gripper link = 0.0705kg; Mass of the Base = 0.950kg

The torque of each servo motor at no load is obtained to be 10kg-cm at 5V Dc input. This is needed to calculate the excess torque the motor has to develop in performing its required task. Moment of inertia is given as [23]:

$$M = arm\ weight \times ½\ arm\ length + motor\ weight\ x\ arm\ weight$$

At the gripper, the torque developed by the servo motor is 10.5 and the excess torque required is determined to be 9.62987 kg-cm. The needed torque at the wrist is calculated to be 0.804125 kg-cm while the excess torque is 9.195875 kg-cm. The needed torque at the elbow is calculated to be 2.76556 kg-cm while the excess torque is 7.23444 kg-cm. The needed torque at the shoulder is 3.12366 kg-cm while the excess torque is 6.87634 kg-cm. The torque required at the base is 3.64666 kg-cm while the excess torque is 6.35334 kg-cm. The maximum torque is taken to be 5 kg-cm giving an allowance of 1.3177 kg-cm. The radius of operation of the mechanism is given as 24.3cm which is the sum of all horizontal link of the mechanism.

4. Dc Servo Motor Modelling

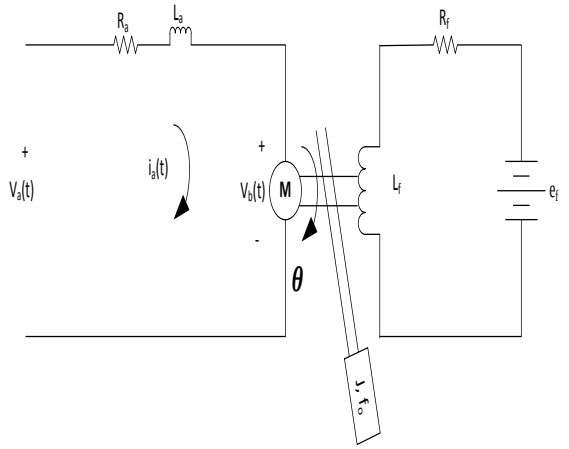

Figure – 5: The DC servo motor circuit diagram [22]

The torque developed by the motor is given as

$$T_m(t) = K_T I_a(t) \tag{36}$$

Taking the friction force to be negligible, the back emf V_b is related to the angular velocity by

$$V_b = K_e W = K_e \frac{d\theta_m}{dt} \tag{37}$$

Kirchhoff's voltage law is applied to the electrical circuit and we have

$$L_a \frac{di}{dt} + R_a i = \varepsilon_a K_e \frac{d\theta_m}{dt} \tag{38}$$

$$\varepsilon_a = i_a R_a + L_a \frac{di_a}{dt} + K_e W_m \tag{39}$$

Equation (40) is obtained after taking the Laplace transform of equation (39)

$$\varepsilon_a = \left(\frac{L_a}{R_a}s+1\right) R_a I_a + K_e W_m \tag{40}$$

Also it should be recalled that $T = K_T I_a = j_T \alpha = j_T W_m s$

$$I_a = \frac{T}{K_T} = \frac{j_T W_m s}{K_T} \tag{41}$$

Substituting Eqns. 41 into 40, we get,

$$\varepsilon_a - K_e W_M = \left(\frac{L_a}{R_a}s+1\right) R_a \frac{j_T W_m s}{K_T} \tag{42}$$

Hence, W_m becomes

$$\frac{(\varepsilon_a - K_e W_M) K_T}{\left(\frac{L_a}{R_a}s+1\right) R_a j_T s} = W_M \tag{43}$$

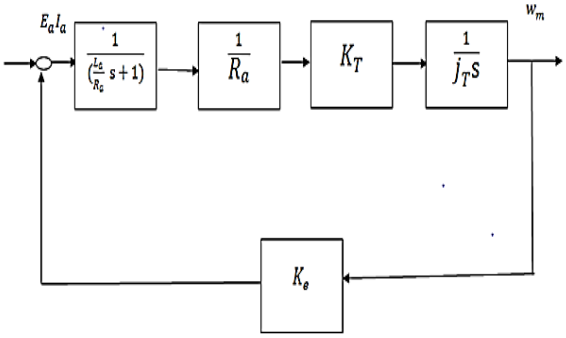

Figure – 6: The Block Diagram of the DC Servomotor.

This closed-loop transfer function of the armature dc controlled motor is obtained from the block diagram of Figure – 6, and Eqns. 44 and 47.

$$\frac{W_m}{\varepsilon_a} = \frac{K_T}{R_a j_T s\left[\left(\frac{L_a}{R_a}\right)s+1\right]+K_e K_T} \quad (44)$$

$$\frac{W_m}{\varepsilon_a} = \frac{K_T}{(R_a j_T \frac{L_a}{R_a})S^2+j_T R_a S+K_e K_T} \quad (45)$$

$$\frac{W_m}{\varepsilon_a} = \frac{K_T}{(j_T L_a)S^2+j_T R_a S+K_e K_T} \quad (46)$$

$$\frac{\theta_m}{\varepsilon_a} = \frac{K_T}{(j_T L_a)S^3+j_T R_a S^2+K_e K_T} \quad (47)$$

For the prototype design operation of the servo Dc motor, the following values are assumed for the servo motor parameters

R_a*(Armature resistance)* = 1.2; L_a *(armature inductance) = 0.07H;* $T_m(t)(motortorque) = 0.7(Nm)$

$$\frac{W_m}{\varepsilon_a} = \frac{1}{(0.3772*0.07)S^2+(0.3772*1.2)s+(1*0.01)}$$

$$\frac{W_m}{\varepsilon_a} = \frac{1}{(0.02640)S^2+0.45264s+0.01}$$

The two above equations are the transfer function for the servo motor at the gripper. So, at the wrist, torque derived earlier is used to calculate the total moment of inertia at the joint, and the value is substituted into the general transfer function of the servo motor. For the second motor at the wrist, the torque calculated is 0.74804kg.cm, converting it to Newton.meter will give

0.804125 x $\frac{9.81}{100}$ = 0.07888Nm

Therefore $j_{load} = \frac{0.07888}{0.12217}$ = 0.6457kg.m^2

For this servo motor j_m = 0. 05kg.m^2

The $j_{total} = j_m + j_{load}$ .Therefore that will yield;

j_{total} = $0.05 + 0.6457kg.m^2$ = 0.6957kg.m^2

The transfer function for the second servo motor is therefore:

$$\frac{W_m}{\varepsilon_a} = \frac{1}{(0.6957*0.07)S^2+(0.6957*1.2)s+0.01} \qquad \frac{W_m}{\varepsilon_a} = \frac{1}{(0.04869)S^2+(0.8348)s+0.01}$$

This is the transfer function for the servo motor at the wrist. For third motor at the elbow, the torque gotten is 2.76556kg.cm, converting it to Newton.meter will give:

2.76556 x $\frac{9.81}{100}$ = 0.2713Nm

Therefore $j_{load} = \frac{0.2713}{0.12217}$ = 2.22068kg.m^2

For this servo motor j_m = 0.05kg.m^2

$j_{total} = j_m + j_{load}$. Therefore, that will yield

j_{total} = 0.05+2.22068kg.m^2 = 2.27068kg.m^2

The transfer function for this third servo motor is therefore:

$$\frac{W_m}{\varepsilon_a} = \frac{1}{(2.27068*0.07)S^2+(2.27068*1.2)s+0.01} = \frac{1}{(0.158947)S^2+2.7248s+0.01}$$

This is the transfer function for the servo motor at the elbow. For the motor at the shoulder, the torque is 3.12366kg.m^2, converting it to Newton.meter will give:

3.12366 x $\frac{9.81}{100}$ = 0.30643Nm

Therefore $j_{load} = \frac{0.30643}{0.12217}$ = 2.5082kg.m^2

For this servo dc motor j_m = 0.05kg.m^2.

The $j_{total} = j_m + j_{load}$. Therefore that will yield;

$j_{total} = 0.05 + 2.5082 \text{kg}.m^2 = 2.5582 \text{kg}.m^2$

The transfer function for this fourth servo motor is therefore:

$$\frac{W_m}{\varepsilon_a} = \frac{1}{(2.5582 * 0.07)S^2 + (2.5582 * 1.2)s + 0.01} = \frac{1}{(0.179074)S^2 + 3.06984s + 0.01}$$

The following Fgure – 7 shows the transfer function for the servo motor at the shoulder.

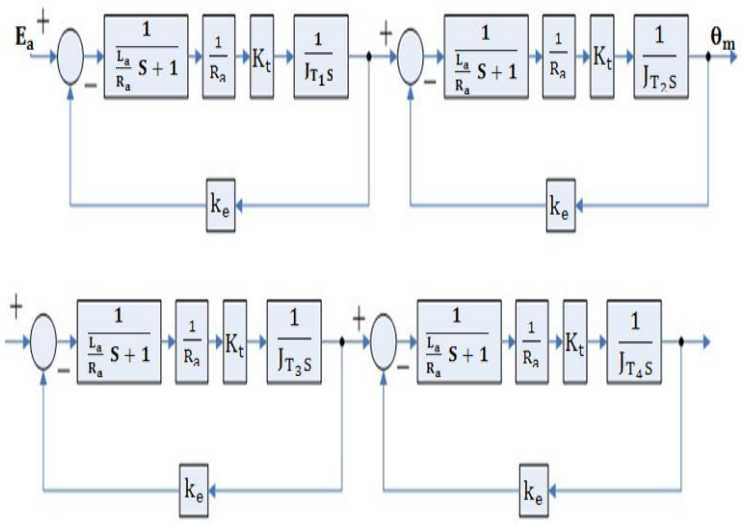

Figure – 7: Block Diagram of the Transfer Function

5. Software Development

As shown in the Figure – 8. the electronic design for this mechanism involves the use of the two Arduino Atmega 283 microcontroller. It is an 8bit microcontroller and the first step involves configuring the register of the Arduino Atmega 283 to work with the desired pulse width modulation technique used.

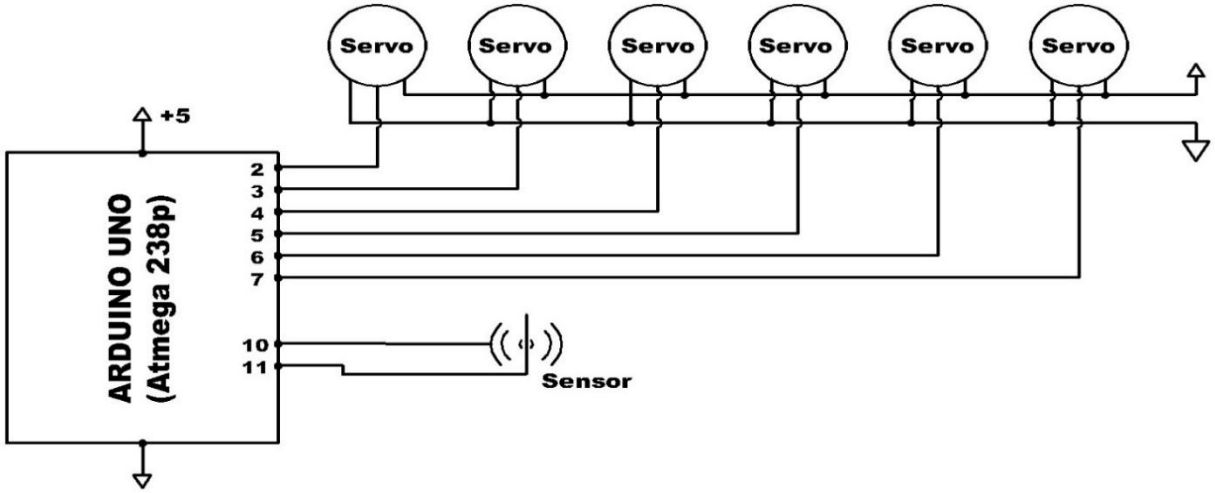

Figure – 8: Electrical Design for the System

6. System Stability

The transfer function is derived from Matlab simulation of servo motors of the equation for the four degree of freedom (Dof) which brings about system stability [23, 24]. The transfer function is expressed as:

$$= \frac{1}{3.659e^{-5}s^8 + 0.002509s^7 + 0.06455s^6 + 0.7388s^5 + 3.183s^4 + 0.1298s^3 + 0.001621s^2 + 7.082e^{-6}s + 1e^{-8}}$$

7. Results And Discussion

The matrices in Figure – 9 were generated for the state space form.

```
>> controlability=ctrb(A,B)
controlability =
   1.0e+10 *
    0.0000   -0.0000    0.0000   -0.0000    0.0003   -0.0083    0.2124   -5.1938
         0    0.0000   -0.0000    0.0000   -0.0000    0.0003   -0.0083    0.2124
         0         0    0.0000   -0.0000    0.0000   -0.0000    0.0003   -0.0083
         0         0         0    0.0000   -0.0000    0.0000   -0.0000    0.0003
         0         0         0         0    0.0000   -0.0000    0.0000   -0.0000
         0         0         0         0         0    0.0000   -0.0000    0.0000
         0         0         0         0         0         0    0.0000   -0.0000
         0         0         0         0         0         0         0    0.0000
>> N=rank(controlability)
N =
     4
>>
```

Figure – 9: The controllability matrix and the rank of matrix

Figure – 10 shows that the controllability matrix rank is incomplete. A complete rank shoud have the value of the rank is equal to the value of the coulumn or row of a square matrix. The controllable matrix for this mechanism is an 8 x 8 matrix and the rank is 4 meaning the rank is not full hence it is not controllable.

```
>> observability=obsv(A,C)
observability =
   1.0e+04 *
         0         0         0         0         0         0         0    2.7330
         0         0         0         0         0         0    2.7330         0
         0         0         0         0         0    2.7330         0         0
         0         0         0         0    2.7330         0         0         0
         0         0         0    2.7330         0         0         0         0
         0         0    2.7330         0         0         0         0         0
         0    2.7330         0         0         0         0         0         0
    2.7330         0         0         0         0         0         0         0
>> M=rank(observability)
M =
     8
```

Figure – 10: The Observability Matrix and the Rank of Matrix

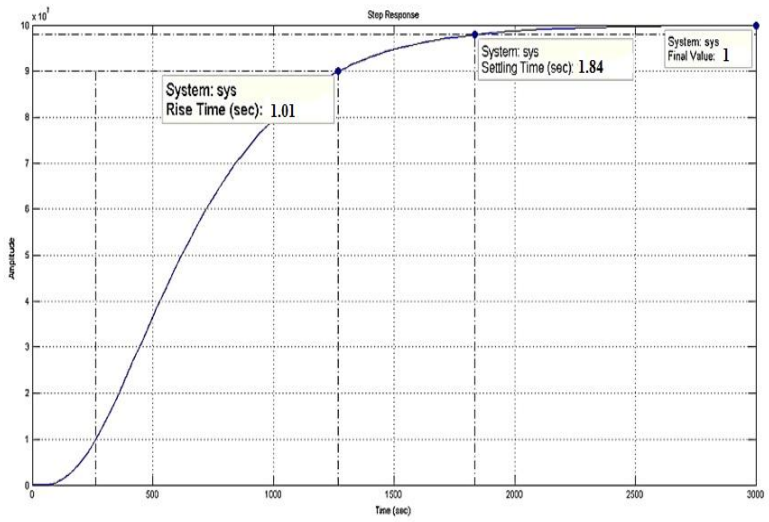

Figure – 11: The Step Response Plot Showing the Value of the Step Information

Figure – 11 shows the step response of the transfer function of the system is displayed. The rise time of the system is 1.01e + 03secs and the settling time is 1.84e + 03secs. The system steady state is at 1e + 08secs. This is considered good for the system.

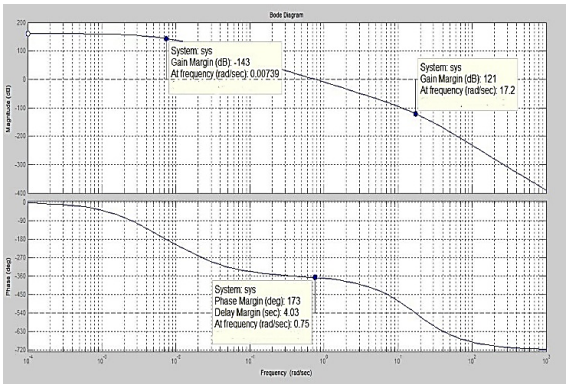

Figure – 12: The Bode Plot for the System

The plot in Figure – 12 shows that the system has a phase margin of 173^0 at a gain crosses frequency of 0.75rad/secs. The point on the plot where the curve crosses 0dB is said to be the phase margin and that which crosses 180dB on the phase plot is said to be the gain margin. The point on the phase plot that the curve crosses -180^0 is traced up to the magnitude plot and the corresponding point on the magnitude plot curve is the gain margin. The phase plot crosses -180^0 at the phase crossover frequency at 0.75 rad/secs when the gain margin is -143dB.

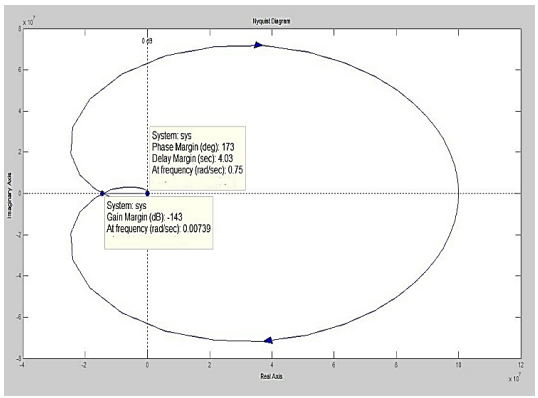

Figure – 13: The system's polar plot

The Figure – 13 shows the polar plot that the phase Margin gotten from the bode plot is 121^0. The gain Margin of the polar plot is also the same as that of the bode plot and it is -143^0. The result from the plot illustrates that the configuration is reliable.

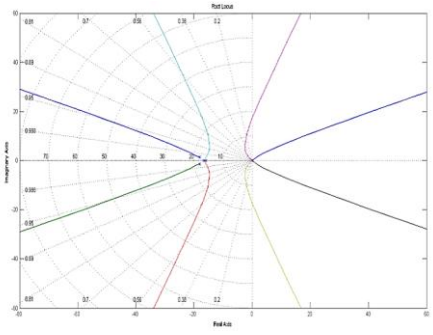

Figure – 14: The Root Locus Plot

The root locus has its zeros on the left-hand side of the plot as shown in Figure – 14 which imply that the system is more stable and speeds up the settling time of the system response.

8. Conclusion

The robotic arm developed performs tasks better in terms of speed and accuracy, and can as well perform a difficult task. Since there is limited muscle activity in the hands of the client, the device can work effectively in unhealthy or impractical locations. The pick and place robot development involves the use of microcontroller and the C-programming language for programming the Arduino with the servo motor controls, and the stability of the system was carried out using a step input signal being a type zero system for easy automation of the system, which makes the device more stable, and reliable, which will also boost productivity when implemented in the industries.

9. References

[1] Zunt, D.(2007). 'Who did actually invent the word "robot" and what does it mean? The Karel Capek website'. Retrieved from http://capek.misto.cz/english/robot.html (Accessed Oct. 10, 2022).

[2] Myint KM, Htun MZ, Htun M, Tun HM, 'Position Control Method for Pick and Place Robot Arm for Object Sorting System', *Int. J. Sci. Technol. Res.*, vol. 5, no. 06, pp. 57–61, 2016. Retrieved from: https://www.ijstr.org/researchpaperpublishing.php?month=june2016 (Accessed Oct. 10, 2022).

[3] Mourya R, Shelke A, Satpute S, Kakade S, Botre M, 'Design and Implementation of Pick and Place Robotic Arm', *Int. J. Recent Res. Civ. Mech. Eng.*, vol. 2, no. 1, pp. 232–240, 2015. Retrieved from https://www.paperpublications.org/issue/IJRRCME/Issue-1-April-2015-September-2015 (Accessed Oct. 10, 2022).

[4] Rajendren B, 'Design and Implementation of multi handling Pick and Place Robotic Arm', *Int. J. Eng. Trends Technol.*, vol. 33, no. 3, pp. 164–166, 2016. https://doi.org/10.14445/22315381/IJETT-V33P230

[5] Harish K, Megha D, Shuklambari M, Amit K, Jambotkar CK, 'Pick and Place Robotic Arm Using Arduino', *Int. J. Sci. Eng. Technol. Res.*, vol. 6, no. 12, pp. 1568–1573, 2017. Retrieved from https://www.researchgate.net/profile/Chaitanya_Jambotkar2/publication/332565132_Pick_and_Place_Robotic_Arm_Using_Arduino/links/5cbefd584585156cd7ab8d03/Pick-and-Place-Robotic-Arm-Using-Arduino.pdf (Accessed Oct. 10, 2022).

[6] Aladetola OD, Akingbade KF, Adelakun NO, 'Development of a Two Link Robotic Manipulator', *Iconic Research and Engineering Journals*, vol. 3, no 8, pp 13-21, 2020. http://doi.org/10.5281/zenodo.3930546

[7] Kumar SS, 'Design of Pick and Place Robot', *Int. J. Adv. Res. Electr. Electron. Instrum. Eng.*, vol. 4, no. 6, pp. 4887–4898, 2015, Available from: https://doi.org/10.15662/ijareeie.2015.0406112.

[8] Sunil T, Famil S, Bhagyesh AVS, Althaf S, 'Design and fabrication of pick and place robotic arm', *2nd Natl. Conf. Recent Trends Mech. Eng. GIST, Nellore. Des.*, pp. 16–26, 2020. Retrieved from https://www.researchgate.net/publication/343738510_Design_and_fabrication_of_pick_and_place_robotic_arm (Accessed Oct. 10, 2022)

[9] Nehmzow U, 'Mobile Robotics: a practical introduction', *UK Springer*, 2003. https://link.springer.com/book/10.1007/978-1-4471-0025-6

[10] Niku SB, 'Introduction to Robotics: Analysis, Control, Applications', 3rd Edition, John Wiley Sons, USA, 2019. https://studylib.net/doc/25750478/introduction-to-robotics-analysis--control--applications ISBN: 978-1-119-52760-2

[11] Lin IH, Liu CY, Chen LC, 'Evaluation of Human-Robot Arm Movement Imitation', *Proc. 8th Asian*

Control Conf., pp. 287–292, 2011. Retrieved from https://ieeexplore.ieee.org/document/5899086 (Accessed Oct. 10, 2022).

[12] Muir FP, Neuman PC, 'Pulsewidth Modulation Control of Brushless DC Motors for Robotic Applications', *IEEE Trans. Ind. Electron.*, vol. 3, no. 32, pp. 222–229, 1985. https://doi.org/10.1109/TIE.1985.350162

[13] Manjula V, RI K, 'Automatic Pick and Place Robot Manipulation Using a Microcontroller Applied & Computational Mathematics Automatic Pick and Place Robot Manipulation Using a Microcontroller', *J. Appl. Comput. Math. Manjula*, vol. 7, no. 3, pp. 1–8, 2018, Available from: Available from: https://doi.org/10.4172/2168-9679.1000408

[14] Surati S, Hedaoo S, Rotti T, Ahuja V, Patel N, 'Pick and Place Robotic Arm: A Review Paper', *Int. Res. J. Eng. Technol.*, vol. 8, no. 2, pp. 2121–2129, 2021. Available from: https://irjet.org/volume8-issue02

[15] Bhalerao A, Doifode P, Chopade K, Gaikwad J, 'Pick and Place Robotic ARM using PLC', *Int. J. Eng. Res. Technol.*, vol. 8, no. 08, pp. 667–670, 2019. Available from: https://doi.org/10.17577/IJERTV8IS080268

[16] Ghadge K, More S, Gaikwad P, Chillal S, 'Robotic Arm for Pick and Place Application', *Int. J. Mech. Eng. Technol.*, vol. 9, no. 1, pp. 125–133, 2018. Available from: https://iaeme.com/Home/article_id/IJMET_09_01_016

[17] Baby A, Augustine C, Thampi C, George M, Abhilash A. P, Jose PC, 'Pick and Place Robotic Arm Implementation Using Arduino', *IOSR J. Electr. Electron. Eng.*, vol. 12, no. 2, pp. 38–41, 2017, Available from: https://doi.org/10.9790/1676-1202033841

[18] Nishar, Kumar D, Sekar, Indira, 'Vision Assisted Pick and Place Robotic Arm', *Adv. Vis. Comput. An Int. J.*, vol. 2, no. 3, pp. 9–18, 2015, Available from: https://doi.org/10.5121/avc.2015.2302.

[19] Nones YA, 'Heterogeneous Modeling & Design of a Robot Arm Control System', *Illinois Tech Robot.*, pp. 1–6, 2003. Available from: https://ptolemy.berkeley.edu/projects/chess/projects/ITR/2003/Yordan-NonesPaper.pdf

[20] Sali K, Kolhe S, Paliwal M, 'Auotomatic Pick and Place Robot', *Int. J. Innov. Res. Sci. Eng.*, vol. 2, no. 3, pp. 636–642, 2016. Available from: https://ijirse.com/volume_detail.php?vny=2016-2-3

[21] Park ID, Park C, Do H, Choi T, Kyung J, 'Design and Analysis of Dual Arm Robot Using Dynamic Simulation', *IEEE 10th Int. Conf. Ubiquitous Robot. Ambient Intell.*, pp. 681–682, 2013. Available from: https://doi.org/10.1109/URAI.2013.6677452

[22] RobotWiki., 'Servos', 2014. Available from: http://www.psurobotics.org/wiki/index.php?title=servos (Accessed Jul. 06, 2022).

[23] Marghitu DB, Mechanisms and Robots Analysis with MATLAB®, Springer London, 2009. ISBN: 978-1-84800-390-3 Available from: https://doi.org/10.1007/978-1-84800-391-0

[24] Craig J. J., Introduction to Robotics: Mechanics and Control, 4th Edition, Addison-Wesley, Reading, MA, 2009. ISBN: 978-0133489798. Available from: http://downloadlink.org/p/solutions-manual-for-introduction-to-robotics-mechanics-and-control-4th-edition-by-craig-ibsn-9780133489798